Integration of upward-GPR and Water Content Reflectometry to monitor snow properties

Authors:

A.Godio, B.Frigo, B.Chiaia - Politecnico di Torino (Italy)

M.Maggioni, M.Freppaz (Università di Torino - Italy)

E. Ceaglio, P. Dellavedova (Fondazione Montagna Sicura – Italy)

Corresponding Author:

Alberto Godio DIATI - Politecnico di Torino

alberto.godio@polito.it

Abstract

We adopt upward Ground Penetrating Radar (up-GPR) and Water Content Reflectometry (WCR) sensors to monitor the seasonal behavior of snow density. Up-GPR permitted to observe at a single fixed station the time lapse response of the electromagnetic signal at the main frequency of 1500 MHz, with the antenna radiating upward from the soil toward the snow surface. Measurements have been performed in a test site on Italian Alps (at elevation of about 2100 m a.s.l.) during the winter season 2014-15 at interval of 30 min. The data processing of radar data involved the traveltime picking and the conversion into snow depth and density. WCR measurements have been useful in order to calibrate the radar response and to retrieve information on the presence of liquid water content.

The integration of up-GPR and WCR technology allow us to infer snow high and layering, snow density changes during the winter season and a preliminary estimate of the liquid water content (LWC). For snow in dry condition, we are able to estimate density values through mixing-rules or polynomial formula. Snow density varies during the season in a range between 250-450 kg/m^3; the results are in good agreement with the results of the ground-truth. For snow in wet condition, the residuals of the electrical permittivity, after a trend removal on the original WCR data permitted to estimate a liquid water content in the range between 3-5 %, during some periods of the winter season, according to warmer climate condition.

Snow layering and densification processes are monitored by the response of up-GPR: fast phenomena such as wetting front infiltration can be also pointed out even if they appear challenging if other observation are not available (e.g. monitoring with WCR).

Key-words:

Ground Penetrating Radar, Water Content Reflectometry, Snow density, Snow water content

Introduction

The development of non-invasive methods to monitor the density and water content by means of electromagnetic devices is of great interest, because of their capability to operate in complex logistical condition (slopes, remote areas, extreme weather condition,...). Moreover, the detection and monitoring of the mechanical properties, jointly with the liquid water content, are relevant in the analysis of snow-gliding phenomena. Glide-snow avalanches occur when the entire snowpack glides over the ground until an avalanche releases. Snow gliding processes and glide-snow avalanches are mainly caused when a reduction in friction at the base of the snow cover occur (e.g. Schweizer et al. 2003); this phenomena is related to an increase of liquid water.

Measurement techniques for the liquid water content of snow are well developed and based on the electromagnetic properties, such as Time-domain Reflectometry, Water Content Reflectometry and Ground Penetrating Radar (Koh et al., 1996). Other methods require an open snow pit and thus are destructive.

The electromagnetic properties of snow are relevant because of their sensitivity to density (e.g. Godio and Rege, 2015a, Godio, 2016) and liquid water content (LWC) changes. Moreover, water percolation in snow or the presence of a wet basal layer in the snow cover are potentially (e.g. Godio and Rege, 2015) associated to the triggering of avalanche and local instability phenomena.

Time-domain reflectometry (TDR) allows for non-invasive continuous monitoring of snow properties within the snowpack (e.g. Schneebeli and others, 1998). Water Content Reflectometry (WCR) is based on similar technology of TDR (e.g. Stein, 1997) and can be easily adapted for automatic monitoring of electromagnetic properties of snow (e.g. Godio et al. 2015b).

Ground Penetrating Radar (GPR) is a promising technology for many applications in snow science, and quantitative results on snow stratigraphy based on radar signals referring on the temporal evolution at a specific site, are of great interest in risk avalanche prediction. Ground Penetrating Radar (GPR) is widely adopted to detect the snow depth and snow-water equivalent (e.g. Godio, 2008, Rege and Godio, 2012, Previati et al. 2011, Forte et al. 2013). The method provides an accurate estimate of the snow depth with much less time spent in the field compared to conventional measurements (e.g. Godio and Rege, 2016, Bruland et al., 2000). Pulsed and frequency modulated GPRs are promising methods, even if they require great care in data processing and calibration as the snow depth is estimated from the traveltime of the radar signal. GPR survey is suitable to cover large areas in an accurate and fast way (e.g. Marchand and al. 2001).

The upward Ground Penetrating Radar (up-GPR) is herein adopted to monitor in time lapse modality the snow properties using a single antenna, disposed on the soil and radiating upward (on the snowpack). Up-ward looking GPR is not a novelty in snow monitoring (e.g. Heilig et al, 2009, 2010, Schmid et al., 2014), while TDR and WCR are widely adopted for soil moisture and they can be successfully adopted to estimate and monitor electrical permittivity of snow (e.g. Previati et al. 2011). Otherwise, the integration of GPR and WCR allows us to monitor the time-lapse behavior of snowpack during the winter season by an integrated approach, where WCR data are useful to calibrate the GPR response.

We have installed upward-looking GPR with the objective of continuously monitoring the temporal evolution of the seasonal alpine snowpack and deriving snow stratigraphy information from the radar signals. The radar response is here analyzed according to the analysis of the WCR data. Particularly, we focus on determining the snow height, the amount of new snow, snow settlements and liquid water content.

Materials and Methods

The monitoring of snow properties was performed at the flat-field test site of Sant'Anna, located above Gressoney at 2100 m a.s.l. in the Monte Rosa sky resort area. The area is on the foothill of the glaciers of MonteRosa massif in the Western Italian Alps.

The equipment has been installed in the test site in September, in order to have enough time to calibrate all the devices before the beginning of the winter season (Figure 1).

Particularly the test site was addressed with one up-Ward GPR, with an antenna working at the main frequency of 1500 MHz; the antenna was buried within the soil (see the paragraph on GPR) and the radar cable was protected and sealed within a corrugated pipe in order to avoid damages due to snow load and possible interferences due to liquid water. The radar unit was installed within a plastic box (together with an external battery), and fixed on a vertical rod, inserted into the ground. The power supply for GPR and other electronic devices (datalogger, WCR units, sensors) was guaranteed by two buffer batteries connected to an inverter and powered by a photovoltaic panel

Three WCR probes for estimating (locally) the dielectric permittivity of ground and snow were connected to a datalogger unit by means of coaxial cables (protected by corrugate pipe). One probe was installed directly into the ground; two probes were located at different elevation with respect to the ground level in order to detect the properties of the snow. The datalogger unit was located in the same plastic box of the GPR unit and powered by the inverter-photovoltaic power system.

Moreover, the test site was equipped with sensors to record meteorological and snow-cover properties; we have installed snow height sensors (HS), an ultrasonic gauges and air temperature, and snow temperature. The HS sensors are based on ultrasonic devices which measure the traveltime of an high frequency pulse, as described in a following paragraph. The sensors were located at an elevation of about 2.5 meters above the ground, as depicted in pictures of Figure 2.

The WCR and GPR measurements were performed in the winter season 2014-15. Particularly, the data acquisition refers to the period starting from November to April, with some lack in data because of some malfunctioning of the GPR equipment.

Conventional manual snow profiles according to the methodology suggested by Fierz and others (2009) were conducted on a bi-weekly basis close to the test site. Snow density was determined by taking samples of volume of 100 cm^3 at different depth in a snow pit and weighting them on an electronic scale. For each layer recorded in the snow pit, at least two density samples were taken and averaged (Table 1).

Electromagnetic properties of snow

The snow is considered as a continuous mixture in which the ice and vapor constituents are themselves treated as individual but interacting continua. Snow on the ground is viewed as an un-saturated three-phase granular material comprised of small grains of ice with interstitial pores partially filled by a single vapor. A small fraction (less than 10 % in volume) of porous voids can be filled by liquid water (wet snow). Bradford et al. (2009) provided an overview on the effect of liquid water content on the electrical permittivity of snow; Lundberg and Thunehed (2000) considered the effect of liquid water on the radar signal into the snowpack. Otherwise, the electrical permittivity of dry snow and ice at different temperature and density has been widely reported (e.g. Evans, 1965, Glen and Paren, 1975). In such condition (dry snow), the electromagnetic measurements can be easily and accurately converted into snow density. Particularly GPR survey is suitable to detect snow depth and dielectric permittivity with high resolution, until a depth of several meters (e.g. Previati et al., 2011).

Mixing rules or adapted mixtures rules relate the dielectric permittivity of the mixture with permittivity and fraction of volume of each single phase. For dry snow (two-phases), several relationships between the electrical permittivity and snow density are well established (e.g. Looyenga, 1965), while for wet snow, where a small fraction of liquid water provides a marked increase of electrical permittivity of the mixtures, the relationships are more challenging, because of the complexity to distinguish between the effect of changes of snow density from liquid content on the observed dielectric permittivity.

The radar performances in terms of reflectivity, vertical resolution and penetration depth have been widely discussed in literature (e.g. Godio, 2007, 2009, Previati et al., 2011). From an electrical point of view, the dry-snow can be considered as non-conducting medium; the electromagnetic wave does not suffer of the intrinsic attenuation as it propagates through the snowpack and it can be assimilated to a lossless medium, in such a case, the complex permittivity is equal to the real permittivity. For instance a granular snow at high density (>600 kg m^{-3}) is characterized by a wavelength of 0.2 m (at 1 GHz) and a theoretical vertical resolution of 0.05 m (assuming the vertical resolution equal to 1/4 of the wavelength).

At the interface between two snow layers or between the snowpack and the air, considering a normal plane wave incidence, the reflection (Γ) and transmission coefficient (τ) are:

$$\Gamma = \frac{\eta_2 - \eta_1}{\eta_2 + \eta_1}$$

$$\tau = \frac{2\eta_2}{\eta_2 + \eta_1}$$

where η is the intrinsic impedance (Ohm m) of layers 1 and 2.

When a signal meets a thin snow layer, multiple reflections between the two interfaces limiting this layer could arise. The amplitude of the resulting wave is dependent on the interferences between the reflected waves, which can be constructive or destructive in function of the traveltime into the layer, itself dependant on the thickness and the snow density.

If both geometric and intrinsic attenuations can be neglected, and if the signal is a continuous plane sinusoid, the resulting reflection coefficient ranges between 0 for purely destructive interferences to one or more maxima, for constructive interferences. Considering a thin snow layer (medium 2), embedded into a medium 1, and assuming a thickness *(t)* of the layer comparable to the wavelength in the first medium, an appropriate expression for the reflection coefficient is (Godio, 2009):

$$\Gamma = \frac{\Gamma_{12}\left(1 - e^{i\beta}\right)}{\left(1 - \Gamma_{12}^{2} e^{i\beta}\right)}$$

where

$$\beta = \frac{4\pi t}{\lambda_1}$$

and λ_1 is the wavelength in the snow layer 1. As the wavelength of the signal is related to the wave velocity, it depends on the density of the snow pack, and therefore the reflection coefficient is affected by the density variation.

A detailed description of the relationship between thickness of a thin snow layer and the reflection coefficient at different frequencies is reported in Godio (2009). For a thin high density snow layer (ε = 3) embedded in a softer snow, with a permittivity value equal ε= 2, the trend of reflection coefficient with respect to the frequency is dependent by the thickness of the layer.

In the frequency range from 100 MHz up to 2 GHz, the trend can be assumed linear for very thin layers (t = 5-10 mm). For increasing thickness (e.g. 50-100 mm), the reflection coefficient assumes a sinusoidal behavior with peaks at different frequencies. For instance, a thin layer of 50 mm is characterized by a maximum of reflection coefficient is at 1 GHz. For a thickness of 100 mm, at the reference frequency of 1 GHz, the reflection coefficient is almost null.

As far as the amplitude of the reflection coefficient is concerned, at the frequency of 1 GHz, the values vary from 0.25 for a thin layer of 5 mm, to 0.05 for the layer of 10 mm and to 0.2 for the layer of 50 mm.

Dry snow

For dry snow, a simple relationships between the snow density and the electromagnetic properties yields. The Robin's equation, for instance, is an empirical relationship between density and electrical permittivity (ε) (Kovacs et al. 1995):

$$\varepsilon=(1+0.845\cdot\rho)^2 \qquad [1]$$

where ρ is the specific gravity of firn and ice (with respect to pure ice) and electrical permittivity is the relative value with respect to vacuum (dimensionless).

The technical literature report many variants of mixing models to relate the snow density and dielectric permittivity. The Robin's equation is a simple polynomial fitting of the straightforward Looyenga (1965) formula, which has been widely used for a bi-phasic mixture of snow. A comparison of the validity and drawbacks of different mixing rule is out of the scope of the manuscript, a detailed description of different approaches is well developed in Booth et alii (2013). We just infer a range of density values, according to the limits of accuracy of the adopted method (Looyenga, 1965).

In terms of wave velocity (v) the following relationship yields:

$$v = c/(1+0.845\cdot\rho) \quad [\text{ m/ns }] \quad [\ 2\ ]$$

where c is the wave velocity in vacuum (here in m/ns). In the velocity range of 0.2 m/ns to 0.24 m/ns the specific gravity almost double (from 0.3 to 0.6).

The relationship between the radar traveltime (twt) and the specific gravity becomes:

$$twt = 2d/c\cdot(1+0.845\cdot\rho) \quad [\text{ ns }] \quad [\ 3\ ]$$

where d is the snow depth; finally we estimate the Snow Water Equivalent (SWE) as:

$$SWE = \rho_{ice}/2\cdot 0.845\cdot(c-v)\cdot twt \quad [kg/m^3\ m] \quad [\ 4\ ]$$

Wet snow

Relationships between the electromagnetic parameters and snow properties are usually based on mixing rules, where the bulk electrical permittivity depends on the fraction volume of each single phase: ice as solid phase, gas and free water (e.g. Sihvola, et al. 1985). A polynomial relationship (Denoth, 1994) between electrical permittivity, density and water content is here adopted:

$$\varepsilon_{snow} = 1 + 1.92\ \rho_{snow} + 0.44\ \rho_{snow}^2 + 0.187\ \theta_w + 0.0045\ \theta_w^2 \quad [\ 5\ ]$$

where ε_s is the dielectric permittivity of the snow, ρ_{snow} (g/cm^3) and θ_w (%) are density and water content, respectively. For dry-snow (neglecting the water content), the equation [5] is similar to standard formulation, usually adopted to estimate density values of dry snow (Godio, 2009, Godio and Rege, 2015a). The sensitivity of the electrical permittivity to the water content effect is demonstrated by analysing the behaviour of the formula [5]. An increase of 3-5 % of liquid content provides a relative increase of the electrical permittivity of more than 20-35 %, as discussed in other papers (e.g. Godio, 2016).

When the the water content is negligible in the reference period, we convert the WCR response in density values using formula [1].

WCR data acquisition

Water Content Reflectometer (WCR) measurements are based on a radio-frequency signal (some decades of MHz) traveling along a two/three rod's probes, acting as a transmission lines, and observing the period of the reflected signal. Particularly, our device consists in an electronic circuit embedded in the probe of two stainless steel rods, 30 cm length, connected to a datalogger. The signal velocity is related to the electromagnetic properties of the embedded material; the electrical permittivity of the material is computed from the observed period.

Two WCR sensors were located at elevation + 70 cm (WCR 2) and + 40 cm (WCR 3) above the ground; a third sensor was located 5 cm below the surface to monitor the interaction between the snow pack and soil.

Laboratory calibration of WCR

We measured the WCR's output in air and de-ionized water at different temperatures, to check the temperature dependence of the electrical permittivity water (Hamelin et al., 1998). The tests were performed in a climatic chamber by monitoring the temperature of the water sample with a thermometer model Fluke S4 I. The frequency-dependence of the constituents of the air and ice is herein neglected as Kelleners et al. (2005) suggested; this is admitted in the bandwidth of approximately 175 MHz of the functioning of the adopted sensor.

A correction of the observed WCR period accounts for the temperature effect of water, ice and air components. A polynomial of 2nd degree is used to correct the observed data in the range between 0 and -8 ° C. By considering these effects, the electrical permittivity of water decreases gradually during the freezing phase; at -12 ° C, the (relative) electrical permittivity assumes values close to 3.2; by increasing the temperature, the permittivity slowly decreases up to values of about 3 (at 0 ° C), when the melting is starting. Those values agree with literature data on the electromagnetic response of water below 0 ° C.

GPR data acquisition

The upward Ground Penetrating Radar (up-GPR) is a pulse-type radar with an antenna, at the main frequency of about 1500 MHz, posed on the ground surface and radiating upward on the snow.

The basic principle is the same of the conventional GPR adopted from the surface; we use a transmitter antenna and a receiver one in bi-static configuration with offset of few cm. The antennas were buried into the ground at the beginning of the winter season, and they have been disposed in such a way that the radiation of the electromagnetic energy was oriented from the ground up-ward. During the wintertime, the ground and the antenna were covered by the snow pack; therefore, the radiation energy propagates from the ground into the snow.

A good compromise between resolution and signal quality and penetration depth, is achieved by using (commercial) antennas in the frequency range between 1 - 2 GHz. This range is suitable to operate with good performance up to a snow thickness of about 2-3 meters that has not been reached during the monitored season. In environments with very huge snow accumulation (more than 3 m), the adoption of commercial antennas with lower main frequency, such as 900 MHz, is suggested and offers good performance (e.g. Previati et al. 2011). Snow humidity (moisture content) does not seem an obstacle (at least in that site) because we estimate that a maximum value of less than 10 % in volume of liquid water is filling the pore volume during the melting period. This quantity does not affect the signal quality.

Snow temperature affect the accuracy of evaluating dielectric permittivity, because of the dependence of dielectric to temperature below 0° Celsius.

This must be considered in further research activity.

The system sends a series of pulses every 30 min to get the A-scans and all the traces are gathered to obtain a B-scan, where along the x-axis we indicate the reference time instead of a distance, as in standard acquisition. Because the low attenuation of the electromagnetic waves in the snow, high frequency can be adopted; the installed system operates at the main frequency of 1500 MHz, with a frequency band of approximately 1 GHz.

We extend the monitoring period from November 2014 till April 2015; measurements were performed every 30 min, with a stacking of 256 traces, on a window time of 50 ns and 1024 sampling for each traces. An analog-to-digital converter of 16 bit was adopted. Results were stored in separated files in the internal memory; and then downloaded for subsequent data processing, because of the complexity of handling an effective remote control of the system.

Data processing

The flow chart of the integrated data processing of GPR, WCR and other data is depicted in figure 3. Particularly, the standard data processing of B-scan involves the edit and removal of distortions of the main-bang, filtering of low frequency electronic noise with dewow, applying the background removal to minimize the main bang effect and reduce coherent “horizontal” noise, The background removal has been performed by averaging 5 traces and subtract the results from the B-scan.

We applied a the gain recover procedure to remove the acquisition gain, to apply a divergence compensation, We didn’t introduce the correction for the intrinsic attenuation because of the negligible dissipation effect of electromagnetic energy in the snow (low attenuation coefficient). The band-pass filter removes the unwanted energy out the frequency band of 1000 - 2200 MHz; finally a trace stacking was performed to get a single traces every two hours. (stacking of four A-scan).

Snow surface picking

We adopt a semi-automatic method, which requires manual interaction according to the following steps:

- a phase follower algorithm detects the peak of the same half-cycle, following the signals at the equal phase;
- If two consecutive traces deviated, we checked whether the height of the snow surface changed due to accumulation, settling or melt; this step is performed by comparing the GPR data with the high of snow (HS) given by ultrasonic measurements (in the period of overlap of the two measurements); an rough evaluation on settling and melting phase has been possible thanks to the analysis of temperature data;
- If none of these changes appeared in the recorded weather data, and deviations in the phase sequence occurred (e.g. while surface crusts were persistent or surface melt happened), we neglected phase reversals;
- During strong accumulation and melt events, manual picking is necessary to reset the follower to the correct phase.

Finally, internal layers were picked in a similar way to the procedure of the semi-automated snow surface picking algorithm.

New snow height (NSH)

Ultrasonic sensors are conventional instrument for measuring snow height; they are able to measure the distance to the snow from the surface.

Particularly, the ultrasonic level sensors work by the "time of flight" principle (basically like the GPR…) using the speed of sound. The sensor emits a high-frequency pulse, generally in the 20 kHz to 200 kHz range, and then observes the echo at the snow-air interface. The pulse is transmitted in a cone, usually about 6° at the apex. The pulse is reflected at the level surface (snow) back to the sensor, now acting as a receiver and then to the transmitter for signal processing. A correction of the speed of sound because of the temperature is necessary for an accurate estimate of the distance between the transmitter-receiver sensors and the snow surface. Usually an accuracy of about 2 % is obtained. Data have been acquired every 30 minutes, and recorded in a data logger. A sketch of the installation of the sensors is reported in figure 1.

During a snowfall, snow height increases and the load of the new snow provides for the settlement of the underlying layers. In such a case the new snow height is always underestimated, i.e. the amount of new snow cannot be measured automatically.

The radar, however, still records the reflection of the old snow surface after it was covered by new snow. Therefore by subtracting the two-way travel time of the reflection of the old snow surface from the time of the new snow surface, a more accurate estimation of the fresh snow height can be performed.

The process requires an assumption of the fresh snow density. At the elevation of the test site (above 2 100 m a.s.l.), the density of the new snow is usually in the range of 50-100 kg/m^3. The wave velocity is in the range between 0.263 - 0.274 m/ns; we calculated the new snow height (NSH) using the following equation:

$$NSH = (Twt_1 - Twt_0)*c / 2 (1+0.845 \rho)$$

where c is the wave velocity in vacuum and ρ is the specific gravity of snow with respect of pure ice (assumed equal to 920 kg/m^3), and Twt_1, and Twt_0 are the traveltimes of the "new" reflection and "old" reflection, respectively.

The accuracy in the detection of the NSH depends on the uncertainty in the assumption of snow density and on the accuracy in the picking of the traveltime differences. A conservative estimate assumes the uncertainty in the estimate of traveltime about 0.05 ns. Therefore, the accuracy in the new snow estimate is computed according to the following analysis:

$$\Delta NHS = |\partial NHS/\partial twt|\cdot\Delta twt + |\partial NHS/\partial\rho|\cdot\Delta\rho$$

$$\Delta NHS = c/2 (1 + 0.845 \rho) \Delta twt + (0.845 c dt)/(2 (1+ 0.845 \rho)^2) \Delta\rho$$

where dt = Twt1 - Twt0, and if the upper and lower boundary are considered:

$$NHS^+ = (dt+\Delta t) *c / (2 (1+0.845 (\rho-\Delta\rho))$$

$$NHS^- = (dt-\Delta t) *c / (2 (1+0.845 (\rho+\Delta\rho))$$

For a gravity value of 0.13 with an uncertainty of 0.025, and assuming a differences of traveltimes of 5 ns, and a interval of 0.5 ns, the fresh snow height results:

$$NHS= 0.68+/-0.08 \quad [m]$$

with a relative uncertainty of about 12 %.

Processing of WCR data

The densification process is a long term process that could provide gradual variation of the response in time during the season. Therefore abrupt changes (in time) of the WCR response are mainly related to the effect on the dielectric permittivity of the liquid water content in the snow. Particularly, time series of WCR data are processed by separating the short term oscillations of electrical permittivity from the long term ones, adopting a de-trend analysis, as depicted in figure 4. Finally the water content is estimated from the residual data of the electrical permittivity, through formula [5].

Results and Discussion

WCR data

The seasonal response of WCR data is shown in figure 4. WCR 1 refers to the response of the probe into the soil. WCR2 and WCR3 are the probe at elevation of +40 cm and 70 cm above the ground (on the snow); the data processing of observed electromagnetic response involves two steps: i) the analysis of the time series, ii) the conversion of the electrical permittivity into snow density and liquid water content by applying mixing rules.

We stress the relevancy of monitoring the ground condition, by observing the water content in the uppermost surface soil. We observed all along the season the presence of high water content (almost close to the saturation) and no frozen phenomenon of the soil: this is of interest both for modeling the thermal regime of the snowpack, and for linking different sliding condition of the snowpack at the interface with the ground.

The high frequency oscillations at small amplitude are related to the influence of the diurnal temperature, because the measurements are not compensated by the temperature correction; the effect is more pronounced on the WCR 2 that is closer to the snow-air interface, where the exposure and influence of solar radiation and air temperature is more relevant.

Moreover the trend of the data of WCR 2 indicates a marked increase of the electrical permittivity of the uppermost layer of the snow pack; the observed values are similar to the values assumed for ice. In this case, like for the seasonal data, we can't distinguish if the effect on the electrical permittivity is caused by densification processes or because a increase of free water content is occurred. The density values have been computed according to the formula [1]; the relationships allowed us to convert the dielectric permittivity of the WCR data into snow density values. Particularly, we observe how the uppermost layers are characterized all over the season by density in the range between 250-300 kg/m^3, while at deeper level, density values are around 400-450 kg/m^3. Those ranges are in good agreement with the values observed on samples collected at different time in snow-pits (Table 1). For the density range in those ranges, the wave velocity is between 0.22-0.24 m/ns.

Figure 5 shows a detail of the electrical permittivity response, observed at sensor WCR2, and the de-trend analysis herein adopted in order to separate short-term and long-term oscillations. The residual are used to estimate the liquid content within the snow pack, according to the procedure aforementioned.

GPR data

A general overview of the up-GPR response is depicted din figure 6. We plot the GPR data collected in the period January to April 2015. Unfortunately because of a malfunction of the GPR system some data are missing in February. A qualitative comparison between the GPR data and the measures of snow height collected with the ultrasonic device show a good agreement between the two data sets in terms of estimate of snow accumulation at the ground.

GPR image (figure 7) shows the temporal evolution of the snow depth accumulated at soil; an average value of 0.23 m/ns is adopted to convert the traveltimes in to snow elevation on the ground. This value has been computed according to an estimate of the average dielectric permittivity derived from the WCR data; particularly we have observed an average value all over the season of about 1.6 -/+ 0.1 (1 Standard Deviation) for the probe WCR 2 and 1.8 -/+ 0.1 (1 Standard Deviation) foe WCR 3. This yields to an average estimate of the dielectric permittivity of the snow pack of 1.7 -/+ 0.2; the wave velocity is therefore in the range of 2.2 m/ns and 2.4 m/ns, or 0.23-/+0.1 m/ns. The adopted velocity value correspond to an average density of 350 kg/m^3; this value is consistent with the range of values observed all over the season with locally measurements of snow in snow pit (Table 1).

The radar section shows several phenomena, that have been highlighted with caps letters. Particularly letter A refers to an abrupt decrease of the snow height just after the first snowfall in November. This is caused by a marked increase in the average temperature in that period, responsible both for a rapid snow settlement (compaction), both causing the formation of a basal ice crust (letter B) and probably also a rapid melting of the snow pack occurred. Subsequent snow falls (letter C and D) provided for an abrupt increase of the snow height in the day from 9 to 11 December. Other snow fall events are pointed out with letter E,F.

A sharp increase of reflectivity of the inner features within the snow pack are highlighted with letters B, G and H. Feature B refers to the formation of a basal crust, subsequent to the partial melt and re-frozen of the snow pack at the beginning of December; features G and H are instead located in the uppermost zone of the snow pack, close to air-snow interface. Two different explanations can be given: i) an increase of the humidity of the new snow with respect to the old one provide an increase of the contrast of the electromagnetic properties between new and old snow; ii) the new snow is characterized by very low density, with respect to the older one; this provides an high reflection coefficient between new and old snow but with a reverse sign with respect to the case i). A detailed analysis of the phase behavior could be helpful in better understating the reason of the hot spots of reflectivity is still in progress.

We also observe a gradual decrease of the snow depth after the main snowfalls, according to snow settlement because of the thermal or mechanical densification processes. This is well depicted in figure 7 by analyzing the trend of the air-snow interface, for instance in between event E and F and between F and G.

We note well separated reflection events into the snowpack; the snow layers that are detectable in the radar image refer to layers with different density values within the snow pack. We can outline the event in between features G and H; pointed out with a dashed black line. This event refers to a reflection of a layers into the snowpack, that shows a gently decrease of the snow-high with time. .

Above the snow-air reflection some weaker artifacts can be observed (letter M in figure 7); those artifacts are associated to multiple reflections of the main features (layers) within the snow pack. This is consistent with the similarity of the trend of the artifacts (multiples) and the inner reflectors. The high contrast of dielectric permittivity between the snow pack and the air (2.5 snow, 1 air) explain how some energy can be trapped within the uppermost snow layers, generating the multiple response.

The analysis of the behavior at the end of the season (Figure 8) reveals the relationship of radar signal with the gradual snow melting; particularly, this effect started at the beginning of April and can be observed till the end of April. We note the similar high frequency (daily) fluctuations of the radar signal at snow-air interface, that can be also observed in the snow depth (ultrasonic data). This corroborates the assumption of the relationship between the oscillations of the signals and the partial frozen-and melting phase of water within the snow pack. This phenomena provides for slight but detectable (according to the instrumental accuracy) behavior of the expansion and contraction of the snow pack because of different density of the snow pack during the partial-melting phase and during the re-frozen period. The fluctuations are related to the different densities of the two phases of water.

Our experiment setup is different from that addressed in similar research activity. For instance Schmid et al. (2015) proposed an interesting combination of up-GPR and Global Positioning System devices to monitor snowpack properties. In particular they installed up-GPRand a low-cost GPS system below the snow cover and observed the evolution during two winter seasons. Applying external snow height (HS) information, they demonstrated as both methods provided consistent liquid water content estimates in snow, based on independent measurements of travel time and attenuation of electromagnetic waves. We obtained similar results by integrating up-GPR with WCR information, even if we focus on density evaluation more then on LWC. Moreover, we focus on the behavior of the ground just below the snow cover and we demonstrate (in this case) that the soil has been, during all the winter season in not frozen condition. This has relevant implication for the analysis of water exchange between the ground and the snow pack and also in the evaluation of thermal regime at the snow-ground interface.

Snow depth and temperature

The analysis of snow depth trend from January to April points out the several precipitation events mostly occurred in March (Figure 9). The climate conditions of the site have been responsible of relevant snow falls, followed by abrupt and marked snow settlements We highlight note the event of February, the 5-6th: an accumulation of about a 40 cm of new snow occurred but the day after an abrupt increase of the air temperature provided for a sudden snow settlement (more than 30 cm). This was followed by a few days of stability, with a small reduction of the snow depth (few cm), according to the decrease of the air temperature. This fast snow settlement is also visible in several events in February and March.

The snow settlement appears very sensitive to the diurnal fluctuations of the air temperature, and obviously to the general climate conditions. The response is very fast, with relevant consequence to the probability of an increase of free water content in the uppermost layers of the snow. This could be analysed in detail considering the reflectivity and phase of the radar signal, for instance.

The snow depth reached a maximum values of about 120 cm and then gradually decreased till less than 60 cm at the end of April. Small fluctuations of snow depth can be observed with a daily frequency. We associate this effect to the melting and refrozen of ice-water in the pore space of the snow, that slightly modifies the snow depth.

The snow melting started approximately at the beginning of April; the comparison between the snow depth, collected by ultrasonic measurements, and the air temperature shows the correlation between the average temperature and the snow melting phase. After a last relevant snow fall, occurred during the days April, 5-6th, the average temperature raised up to values above 0° Celsius , with diurnal fluctuations between -5 and + 10 Celsius degree.

Soil water content

The response of WCR in the soil shows a regular and almost constant trend all over the monitoring period. Some small fluctuations could be of interest mostly because they appear well related to the fluctuations observed in the data of WCRs located in the snow (e.g. the event at middle of January).

We note that the values of about 45-55 % of water content are compatible with the nature of the uppermost part of the soil, characterised by a soil with high porosity and low permeability. Therefore a high water content is observed and the soil remains in almost saturated condition for long time. The early snow falls at the end of November provided for a enough thickness of snow cover to avoid the water within the soil to freeze. This condition of unfrozen soil remains for all the winter season.

Final remarks

We have proven that the integration of WCR and GPR response is an effective tool to monitor the seasonal variation of snow properties. For snow in dry condition, we are able to estimate density values through mixing-rules or polynomial formula. The water content is estimated by performing the analysis of the residuals of the electrical permittivity, after a trend removal on the original WCR data.

Snow layering within the snow pack, and densification processes are monitored by upward-GPR: fast phenomena such as wetting front infiltration are of relevant interest but they are challenging if evidences coming from other observation are not available (e.g. monitoring with WCR). Even if an accurate analysis of volumetric water content within the snowpack appears still challenging, we will work on the spatial variability. This will require the development of low cost (simplified, e.g. multiplexing devices) radar system must be developed to drive an array of antennas. WCR is (rather) low-cost devices that can be routinely integrated in snow-weathering stations.

The integration of WCR and up- GPR offers a good accuracy in monitoring the average values of snow density. Moreover upward GPR, WCR probes and conventional snow depth observations permit detailed analysis of snow deposition, the settlement phase, densification process and melting and frozen phase.

The further data processing would focus on the analysis of the observed data with marked variations of snow depth and with an increase of free water within the pore volume of the snow pack. These phenomena, jointly with the analysis of the temperature trend, could be associated to the probability of the occurrence of snow gliding.

Acknowledgements

The research is conducted in the framework of MRTeam project, funded by *Regione Val d'Aosta* - Italy (B 65 G 13000 00 0006).

Table 1: snow depth and density at two different elevation above the ground during the winter 2014-15, observed in pits.

Date	17-Dec	21 - Dec	31 - Dec	7 - Jan	28 - Jan	4 - Feb	12 - Feb	18 - Feb	4 - Mar	11 - Mar
Snow Depth [cm]	80	70	65	64	87	99	110	125	132	113
Density at elevation + 0.7 m [kg/m^3]	120-340	200	-	-	200	260	270	300	320	400-340
Density at elevation + 0.4 m [kg/m^3]	340-420	300-360	320	400	400	400	270	380	400	400

References

Booth A. D., Mercer A., Clark R., Murray T., Jansson P., Axtell C., 2013. A comparison of seismic and radar methods to establish the thickness and density of glacier snow cover. *Annals of Glaciology* 54 (64) , 73-82, doi:10.3189/2013aog64a044

Bradford J.H., Harper J.T. and Brown J., 2009. Complex dielectric permittivity measurements from ground-penetrating radar data to estimate snow liquid water content in the pendular regime. *Water Resour. Res.* , 45 (8), W08403 (doi: 10.1029/2008WR007341)

Bruland O., Sand K., Killingtveit A., 2000. Snow distribution at a high Arctic site at Svalbard. *Nordic Hydrology* 32:, 1–12.

Denoth, A., 1994. An electronic device for long-term snow wetness registration. *Annales of Glaciology*, 19, 104-106.

Evans S. 1965. Dielectric properties of ice and snow. *Journal of Glaciology* 5: 773-792.

Glen J.W, Paren J.G., 1975. The electrical properties of snow and ice. *Journal of Glaciology* 15, 15-38.

Fierz, C., Armstrong, R.L., Durand, Y., Etchevers, P., Greene, E., McClung, D.M., Nishimura, K., Satyawali, P.K. and Sokratov, S.A. 2009. The International Classification for Seasonal Snow on the Ground. IHP-VII Technical Documents in Hydrology N° 83, IACS Contribution N° 1, UNESCO-IHP, Paris.

Forte, E., Dossi, M., Colucci, R.R., Pipan, M., 2013. A new fast methodology to estimate the density of frozen materials by means of common offset GPR data. *Journal of Applied Geophysics*, 99, 135–145.

Forte, E., Pipan, M., Godio, A., Francese R., 2015. An overview of GPR investigation in the Italian Alps. *First Break,* 33, 8, 61-67.

Godio A. 2008. Performance and experimental evidence of GPR in density estimates of snowpack. *Bollettino di Geofisica Teorica e Applicata* 49: 279-298.

Godio A. 2009. Georadar measurements for snow cover density. *American Journal of Applied Sciences* 6 : 414-423.

Godio A., Rege R.B., 2015a. The mechanical properties of snow and ice of an alpine glacier inferred by integrating seismic and GPR methods, *Journal of Applied Geophysics*, 115, 92-99, http://dx.doi.org/10.1016/j.jappgeo.2015.02.017.

Godio A., Franco D., Chiaia B., Frigo B., Dublanc L., Freppaz M., Maggioni M., Ceaglio

E and Dellavedova P. ,2015b. Seasonal Monitoring of Snow Properties by WCR and up-GPR, EAGE Near Surface Geoscience 2015 - 21st European Meeting of Environmental and Engineering Geophysics, Torino

Godio, A., Rege, R.B., 2016 . Analysis of georadar data to estimate the snow depth distribution, *Journal of Applied Geophysics*, 129, 92-100, http://dx.doi.org/10.1016/j.jappgeo.2016.03.036.

Godio, A., 2016. Multi Population Genetic Algorithm to estimate snow properties from GPR data. Journal of Applied Geophysics, 131, 133-144. DOI: 10.1016/j.jappgeo.2016.05.015

Hamelin, J., Mehl, J.B., Moldover, M.R., 1998. The static dielectric constant of liquid water between 275 K and 400 K near the saturated vapor pressure. *International Journal of Thermophysics*, 19, 1359-1380.

Heilig A., Schneebeli M. and Eisen O. 2009. Upward-looking ground-penetrating radar for monitoring snowpack stratigraphy. *Cold Reg. Sci. Technol.*, 59 (2–3), 152–162 (doi: 10.1016/ j.coldregions.2009.07.008)

Heilig A., Eisen O. and Schneebeli M., 2010. Temporal observations of a seasonal snowpack using upward-looking GPR. *Hydrol. Process.* , 24 (22), 3133–3145 (doi: 10.1002/hyp.7749)

Kelleners, T.J., Seyfred, M.S., Blonquist, J.M., Bilskie, J. and Chandler, D.G, 2005. Improved interpretation of water reflectometer measurements in soils. *Soil Sci. Soc. Am. J.* 69, 1684-1690.

Koh G., Yankielun N.E., Baptista A.I., 1996. Snow cover characterization using multiband FMCW radars. *Hydrol. Process.* 10, 1609–1617.

Kovacs A., Gow A.J., Morey R.M., 1995. The in-situ dielectric constant of polar firn revisited, *Cold Region Science and Technology,* 23, 245-256.

Looyenga, H., 1965. Dielectric constant of heterogeneous mixtures. *Physica* , 31, 401-406.

Lundberg A., Thunehed H. Bergstrom J., 2000. Impulse radar snow surveys – influence of snow density. *Nordic Hydrology* , 31, 1-14.

Lundberg A. and Thunehed H., 2000. Snow wetness influence on impulse radar snow surveys: theoretical and laboratory study. *Nord. Hydrol.* , 31 (2), 89–106 (doi:

10.2166/nh.2000.007)

Marchand W.D., Bruland O, Killingtveit A. 2001. Improved measurements and analysis of spatial snow cover by combining a ground based radar system with a differential global positioning system receiver. *Nordic Hydrology,* 32, 181–194.

Previati M., Godio A., Ferraris S., 2011. Validation of spatial variability of snowpack thickness and density obtained with GPR and TDR methods. *Journal of Applied Geophysic*s, 75, 284-293, DOI: 10.1016/j.jappgeo.2011.07.007.

Rege, R.B., Godio, A., 2012. Multimodal inversion of guided waves in georadar data, *Journal of Applied Geophysics*, 81, 68–75, DOI: 10.1016/j.jappgeo.2011.09.021.

Sand K, Bruland O. 1998. Application of georadar for snow cover surveying. *Nordic Hydrology* 29 : 361–370.

Schmid L., Heilig A., Mitterer, C., Schweizer, J., Maurer, H., Okorn R., Eisen O., 2014. Continuous snowpack monitoring using upward-looking ground-penetrating radar technology. J*ournal of Glaciology*, 60, 221, 2014 doi: 10.3189.

Schmid, L., F. Koch, A. Heilig, M. Prasch, O. Eisen, W. Mauser, and J. Schweizer (2015), A novel sensor combination (upGPR-GPS) to continuously and nondestructively derive snow cover properties, *Geophys. Res. Lett.,* 42, 3397-3405, doi:10.1002/2015GL063732.Schneebeli M., Coleou C., Touvier F. and Lesaffre B. 1998. Measurement of density and wetness in snow using time-domain reflectometry. *Ann. Glaciol.*, 26 , 69–72

Schweizer, J., Jamieson, J.B. and Schneebeli, M, 2003. Snow avalanche formation. *Rev. Geophys.*, 41 (4), 1016 (doi: 10.1029/ 2002RG000123)

Sihvola, A., Nyfors, E. and Tiuri, M., 1985. Mixing formulae and experimental results for the dielectric constant of snow*. Journal of Glaciology,* 31, 163–170.

Stein, J., Laberge, G. and Lèvesque, D. 1997. Monitoring the dry density and the liquid water content of snow using time domain reflectometry. *Cold Regions Science and Technology*, 25, 123–136.

Captions

Figure 1: sketch of the test site with position of sensors.

Figure 2: pictures of the test site; a) installation of the equipment; b) winter time at the test site!

Figure 3: flow chart of the data processing and data integration between GPR and WCR.

Figure 4: winter season 2014-2015, seasonal behavior of WCR response, a) WCR 1 refers to soil water content; b) WCR2 and WCR3 are the probe at elevation of +40 cm and 70 cm above the ground (on the snow).

Figure 5: a) example of de-trend analysis to separate the short term effect and the long term behavior of WCR data; the residuals of the dielectrical permittivity (short term behavior) are related to the effect of the liquid water content.

Figure 6: a) up-ward GPR response, period January 2015 - April 2015; blank sectors refer to data missing; b) snow depth by ultrasonic measurements (data missing in the period January-February 2015).

Figure 7: detail of up-ward GPR response in December2014 , letters A refers to an abrupt compaction and or melting of the snow pack; C,D E,F, refer to the radar response to the new snow falls, features B, G,H are hot spot of reflectivity within the snowpack, N indicates artifact because of multiple reflections. (see the text for further explanations).

Figure 8: a) detail of up-ward GPR response during April; the reflection vent of air-snow interface show some pulsation; a similar behavior is depicted by the ultrasonic response (snow height), in figure b).

Figure 9: Air temperature trend and snow depth according to ultrasonic data during the final snow melting (March-April); the air temperature data are filtered with a low pass filter to enhance the diurnal variation of snow.

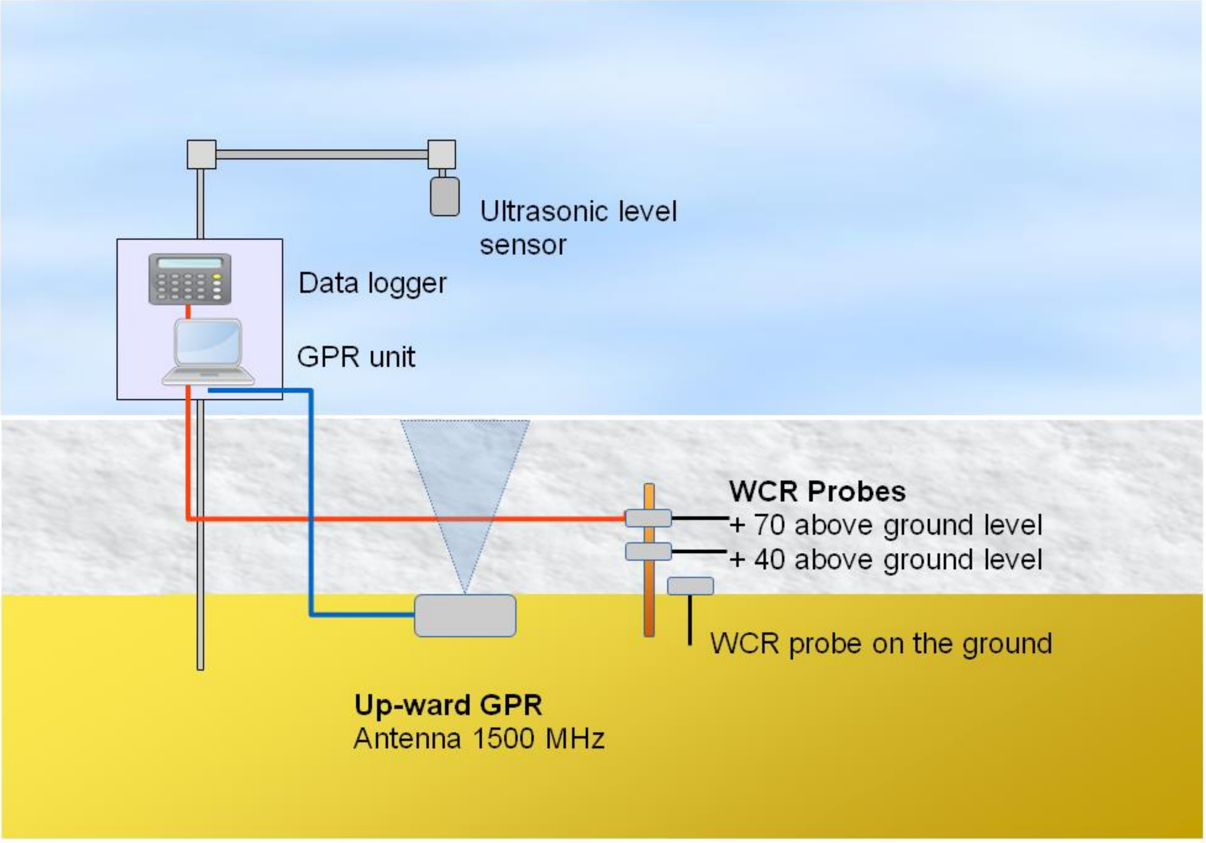

720
721 Figure 1
722

a) b)

Figure 2

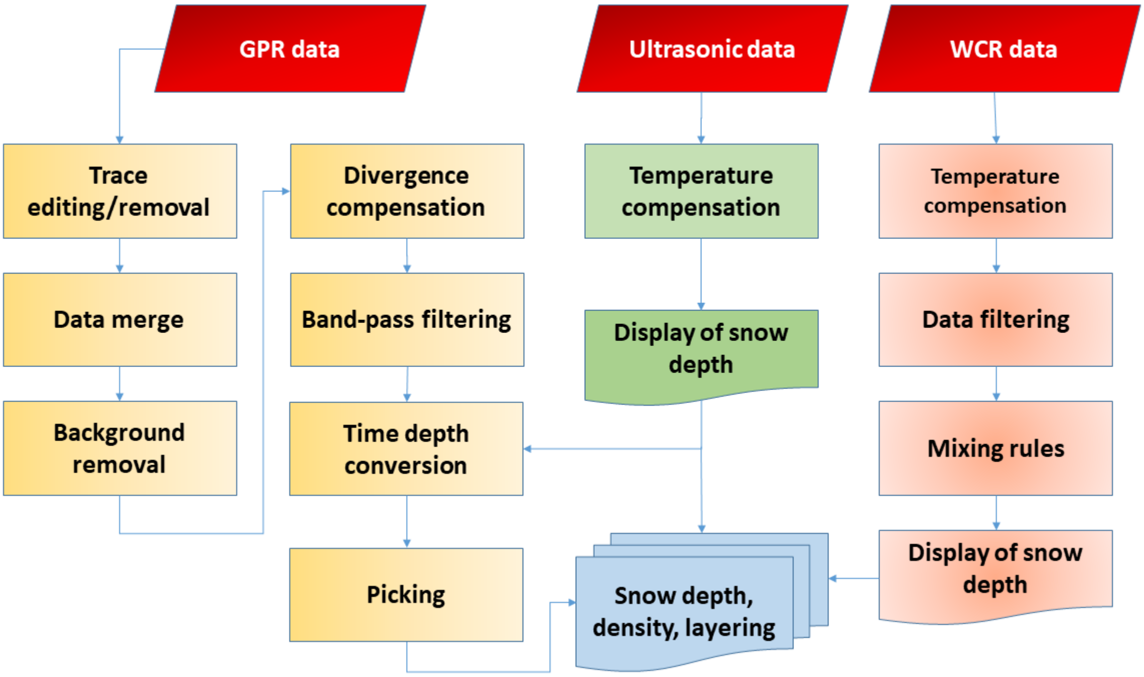
GPR data
Ultrasonic data
WCR data
Trace editing/removal
Divergence compensation
Temperature compensation
Temperature compensation
Data merge
Band-pass filtering
Display of snow depth
Data filtering
Background removal
Time depth conversion
Mixing rules
Picking
Snow depth, density, layering
Display of snow depth

Figure 3

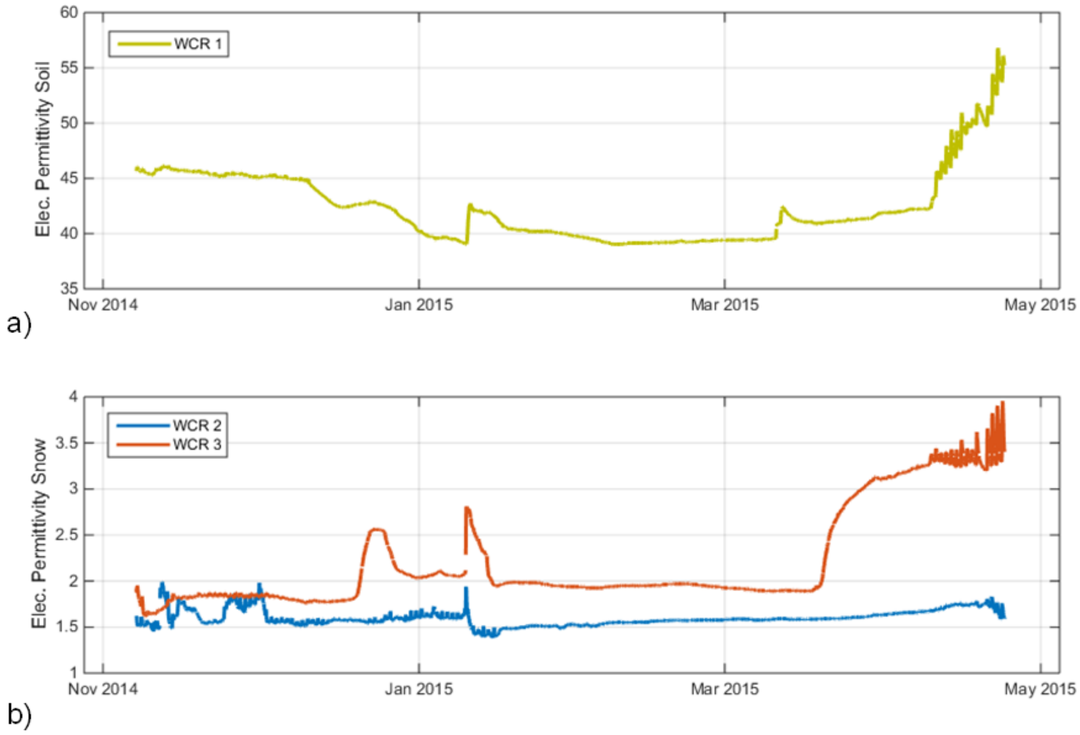
WCR 1
Elec. Permittivity Soil
60
55
50
45
40
35
Nov 2014
Jan 2015
Mar 2015
May 2015
a)
WCR 2
WCR 3
Elec. Permittivity Snow
4
3.5
3
2.5
2
1.5
1
Nov 2014
Jan 2015
Mar 2015
May 2015
b)

Fugure 4

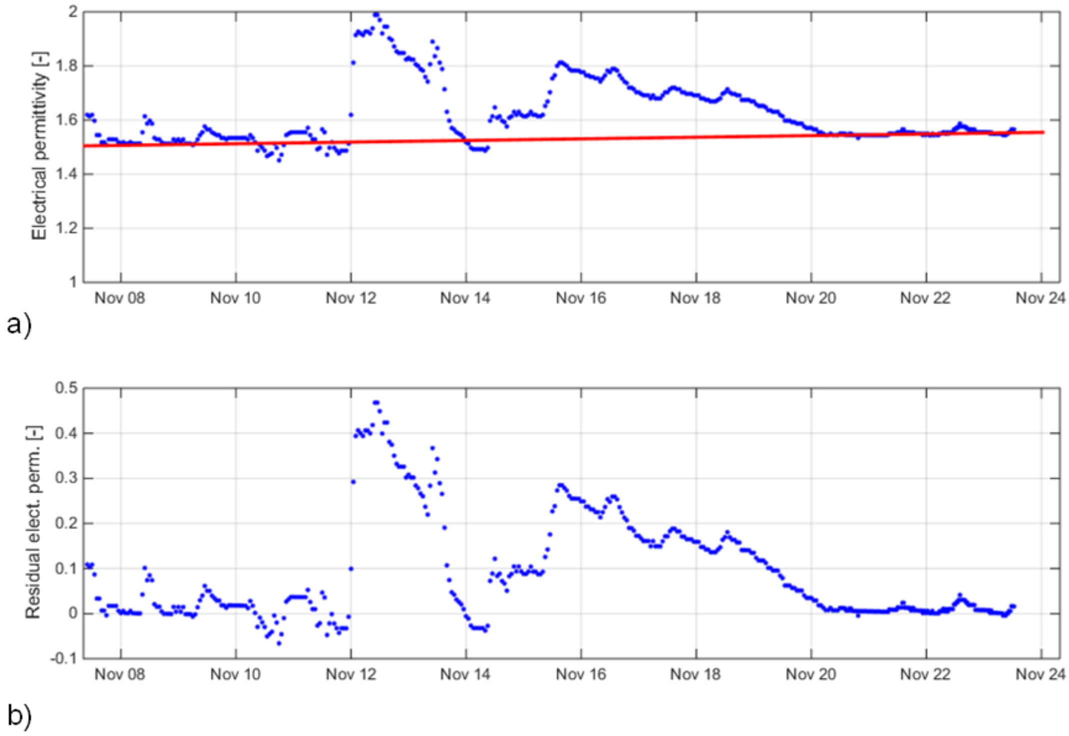
Electrical permittivity [-]
2
1.8
1.6
1.4
1.2
1
Nov 08
Nov 10
Nov 12
Nov 14
Nov 16
Nov 18
Nov 20
Nov 22
Nov 24
a)
Residual elect. perm. [-]
0.5
0.4
0.3
0.2
0.1
0
-0.1
Nov 08
Nov 10
Nov 12
Nov 14
Nov 16
Nov 18
Nov 20
Nov 22
Nov 24
b)

Figure 5

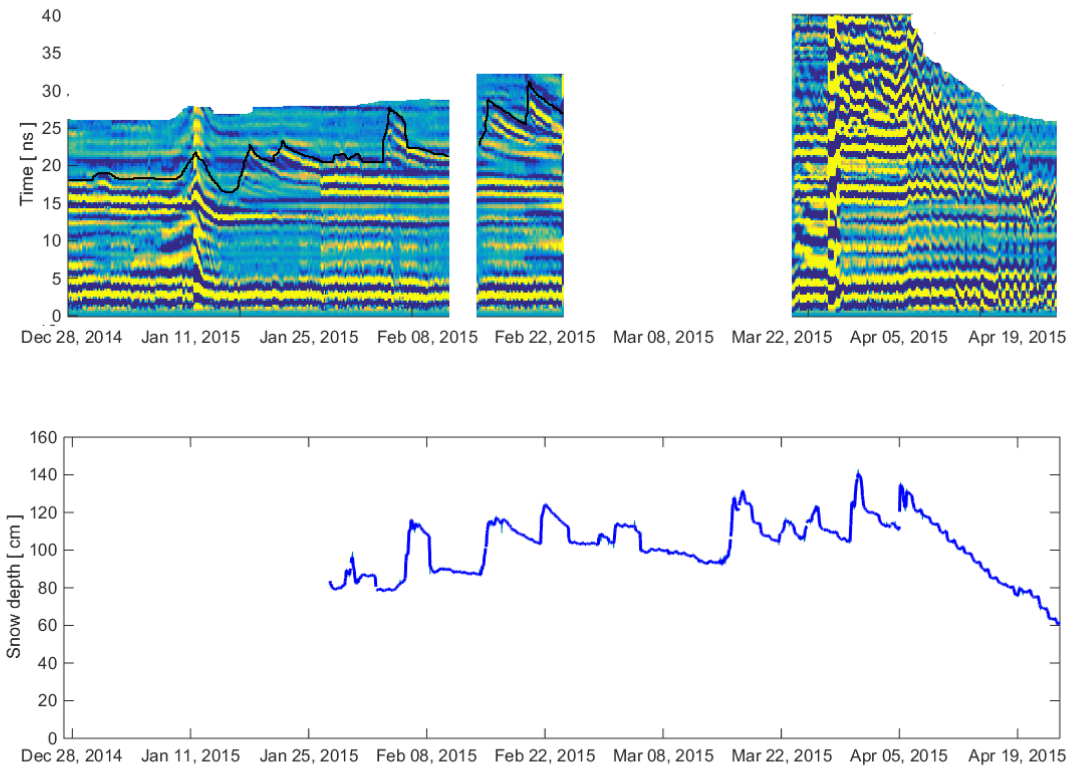

Time [ns]
0
5
10
15
20
25
30
35
40
Dec 28, 2014
Jan 11, 2015
Jan 25, 2015
Feb 08, 2015
Feb 22, 2015
Mar 08, 2015
Mar 22, 2015
Apr 05, 2015
Apr 19, 2015
Snow depth [cm]
0
20
40
60
80
100
120
140
160
Dec 28, 2014
Jan 11, 2015
Jan 25, 2015
Feb 08, 2015
Feb 22, 2015
Mar 08, 2015
Mar 22, 2015
Apr 05, 2015
Apr 19, 2015

Figure 6

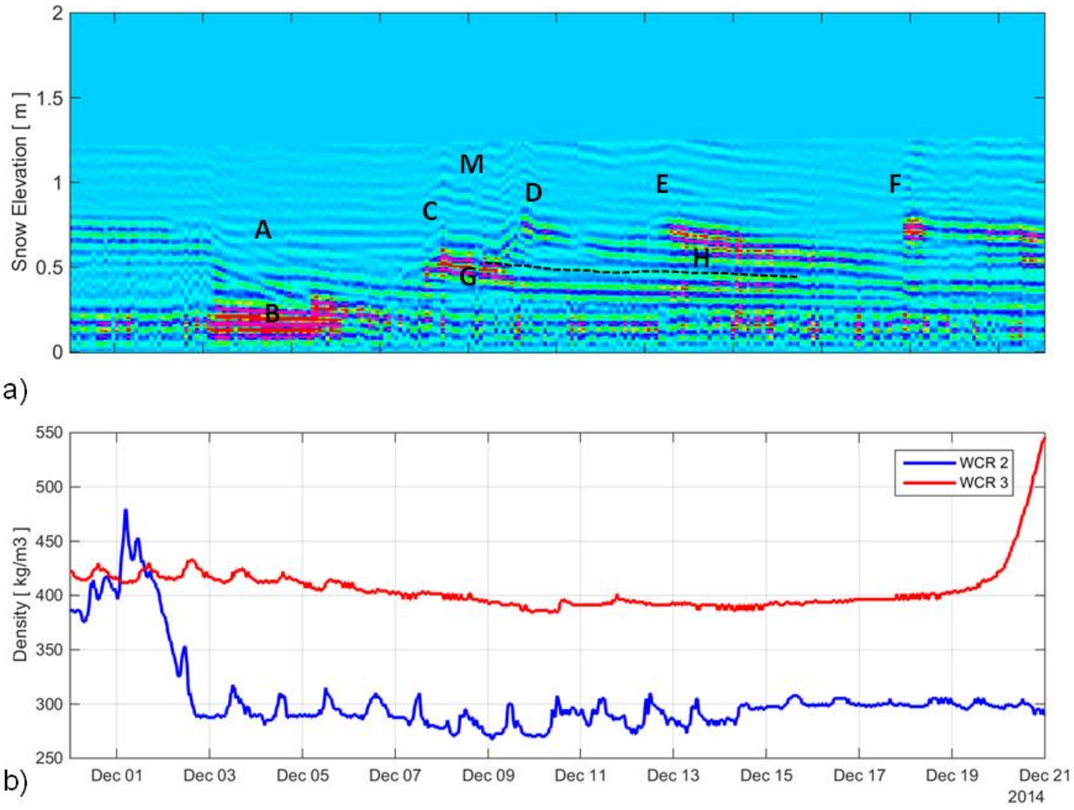

Snow Elevation [m]
2
1.5
1
0.5
0
A
B
C
M
G
D
E
H
F
a)
Density [kg/m3]
550
500
450
400
350
300
250
WCR 2
WCR 3
Dec 01
Dec 03
Dec 05
Dec 07
Dec 09
Dec 11
Dec 13
Dec 15
Dec 17
Dec 19
Dec 21
2014
b)

Figure 7

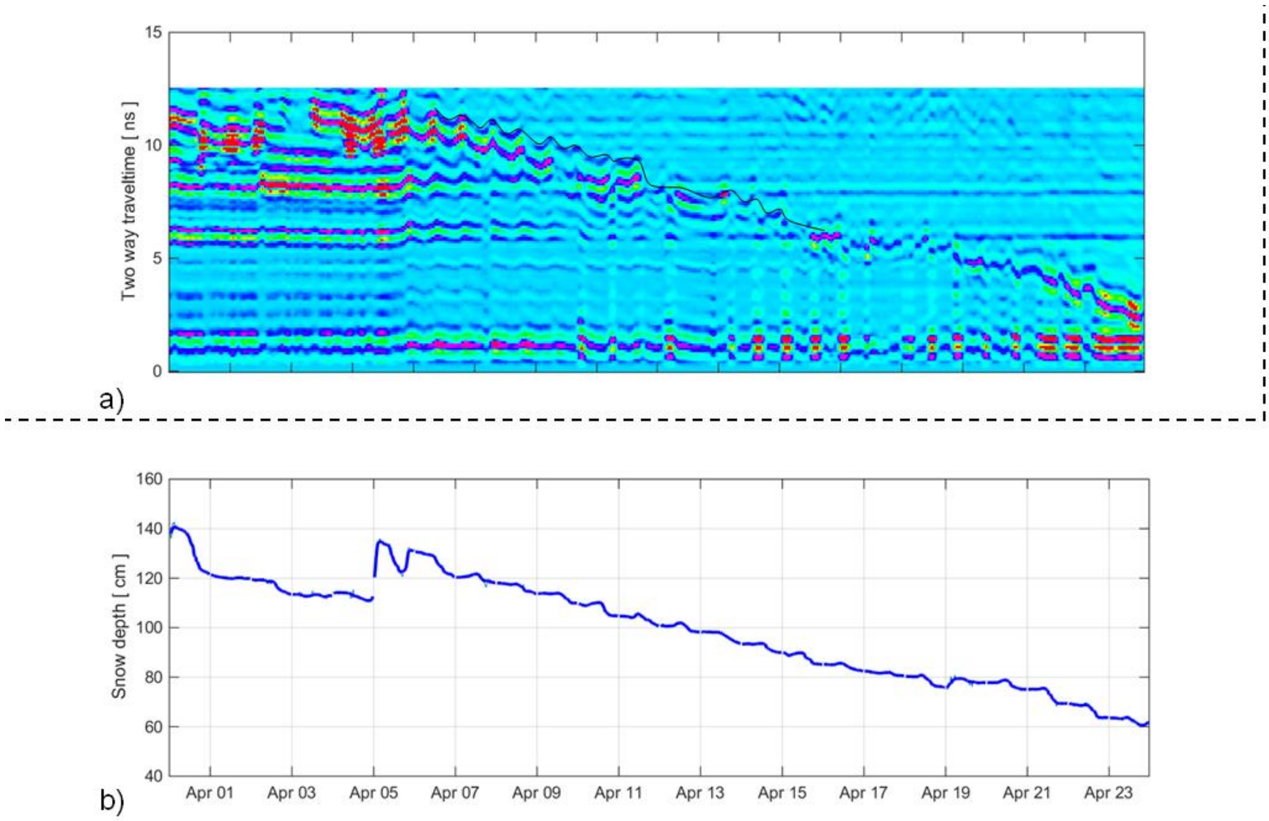

Two way traveltime [ns]
15
10
5
0
a)
Snow depth [cm]
160
140
120
100
80
60
40
Apr 01
Apr 03
Apr 05
Apr 07
Apr 09
Apr 11
Apr 13
Apr 15
Apr 17
Apr 19
Apr 21
Apr 23
b)

Figure 8

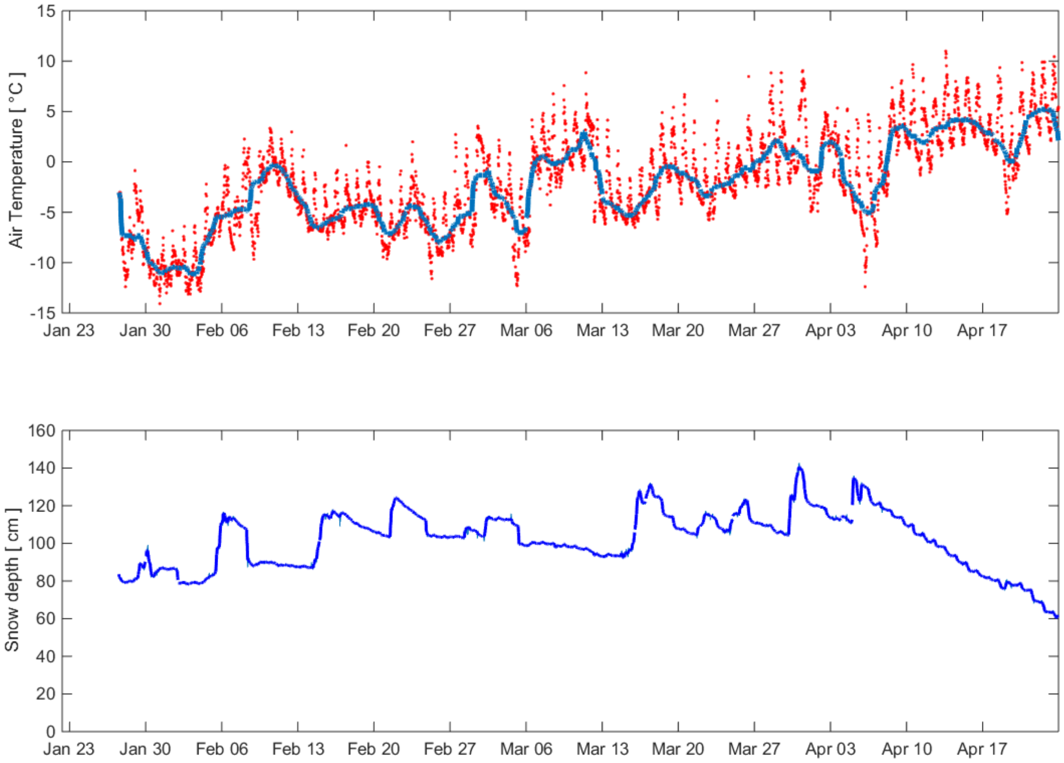
Air Temperature [°C]
15
10
5
0
-5
-10
-15
Jan 23
Jan 30
Feb 06
Feb 13
Feb 20
Feb 27
Mar 06
Mar 13
Mar 20
Mar 27
Apr 03
Apr 10
Apr 17
Snow depth [cm]
160
140
120
100
80
60
40
20
0
Jan 23
Jan 30
Feb 06
Feb 13
Feb 20
Feb 27
Mar 06
Mar 13
Mar 20
Mar 27
Apr 03
Apr 10
Apr 17

Figure 9